

Flying batteries: In-flight battery switching to increase multirotor flight time

Karan P. Jain and Mark W. Mueller

Abstract—We present a novel approach to increase the flight time of a multirotor via mid-air docking and in-flight battery switching. A main quadcopter flying using a primary battery has a docking platform attached to it. A ‘flying battery’ – a small quadcopter carrying a secondary battery – is equipped with docking legs that can mate with the main quadcopter’s platform. Connectors between the legs and the platform establish electrical contact on docking, and enable power transfer from the secondary battery to the main quadcopter. A custom-designed circuit allows arbitrary switching between the primary battery and secondary battery. We demonstrate the concept in a flight experiment¹ involving repeated docking, battery switching, and undocking. The experiment increases the flight time of the main quadcopter by a factor of $4.7\times$ compared to solo flight, and $2.2\times$ a theoretical limit for that given multirotor. Importantly, this increase in flight time is not associated with a large increase in overall vehicle mass or size, leaving the main quadcopter in fundamentally the same safety class.

I. INTRODUCTION

Multirotors are frequently employed in mapping, delivery, monitoring, search and rescue missions [1]–[3] among many other applications owing to their ability to hover. However, multirotors inherently have lower endurance and range as compared to fixed-wing aircraft [4]. There is a growing demand for higher endurance and range in multirotors with their increasing usage in the research, commercial and industrial setting.

Current literature covers innovative methods to increase the endurance of multirotors. A hybrid aerial vehicle is presented in [5] which exploits the efficiency of a fixed-wing and hovering ability of a multirotor. An online strategy for optimizing efficiency by altering flight parameters over a trajectory is presented in [6]. An interesting approach without attempting to increase efficiency is to have a ‘refueling’ station for a quadcopter. Battery recharging is demonstrated in [7]. However, it is a slower process as compared to conventional refueling. This is resolved by instead performing a battery swap where a discharged battery is swapped with a charged one. Battery swapping at a ground station has been shown in [8]–[10]. One limitation of ground-based swapping stations is an interruption to the mission. For example, if a quadcopter’s mission is monitoring a target, then going to a ground station for battery replacement results in a mission failure. A spare battery having the ability to come to the quadcopter instead of the other way around

will enable an uninterrupted mission. This capability can be enhanced if the spare battery can be removed in-flight after discharging so that another spare battery can take its place and continue providing energy. Moreover, this would allow a system to operate for long-distance flights without the disruption of stopping the flight, potentially a crucial feature to applications such as urban air mobility.

We present the concept of a ‘flying battery’ – a secondary battery that is mounted on a small quadcopter. While a main quadcopter is performing some task mid-air using a primary battery, a flying battery can fly towards the main quadcopter and dock on it. The main quadcopter can then switch its power source to the secondary battery. Once the secondary battery is depleted, the flying battery can undock, and another fully charged flying battery can dock in its place. This process can be repeated until the primary battery is depleted. The primary battery is only used from the time when one flying battery undocks until another one docks back. This increases the total flight time and is achieved while the main quadcopter is airborne, so there is no interruption to the mission. Fig. 1 shows a flying battery approaching the main quadcopter to dock on it.

The paper is organized as follows. Section II presents a fundamental flight time vs. battery mass analysis to motivate the usage of our proposed system. Section III explains the hardware design of our system. Section IV covers the method of docking a flying battery on the main quadcopter and undocking it. Section V demonstrates how our design increases the flight time of the primary quadcopter.

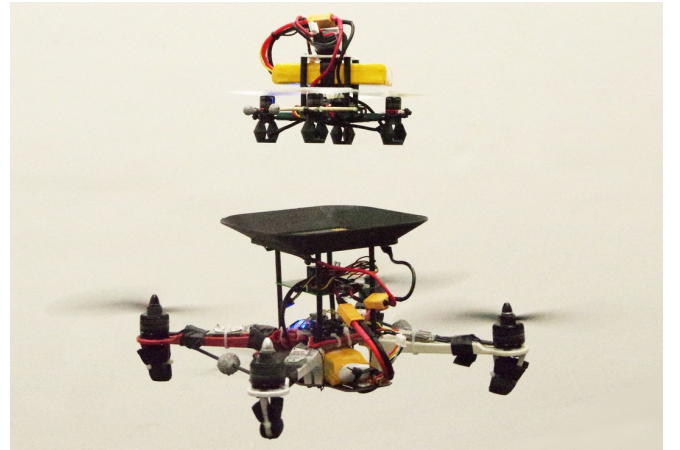


Fig. 1: A flying battery (above) about to dock on the main quadcopter (below).

Authors are with the High Performance Robotics Laboratory (HiPeRLab) at the Department of Mechanical Engineering, UC Berkeley, CA 94720, USA. {karanjain, mwm}@berkeley.edu

¹The explanation and experimental validation video can be found here: <https://youtu.be/P6XvhTe1Rdo/>

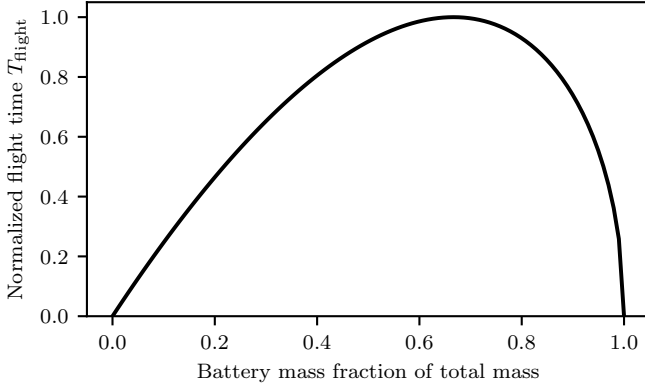


Fig. 2: Effect of battery mass on hovering flight time, showing a peak at $\phi = \frac{2}{3}$, after which adding a larger battery results in reduced flight time.

II. MOTIVATION

In this section, we present an analysis of a fundamental limitation of hovering battery-powered multirotors. Specifically, we show that the achievable flight time only increases up to a certain point, as more battery is used on a vehicle.

Following the analysis of [11], [12], we model the aerodynamic power consumption p_i of an individual propeller i to be related to that propeller's thrust f_i as

$$p_i \propto f_i^{\frac{3}{2}} \quad (1)$$

This result can be derived from actuator disk theory [12], or from mechanical analysis of hub torque and rotational speed [11].

For a hovering multirotor, the individual propeller thrusts scale proportionally with the vehicle's total mass. The available flight time T_{flight} can be related to the battery capacity E_{batt} and electric power draw p_{elec} as

$$T_{\text{flight}} = \frac{E_{\text{batt}}}{p_{\text{elec}}} \quad (2)$$

Under a constant specific energy assumption, the total available energy in a battery will be proportional to the battery's mass. Let m_0 be the mass of all components of the multirotor, excluding the battery, and let ϕ be the fraction of the *total* vehicle mass that is the battery mass, so that the total vehicle mass is $\frac{1}{1-\phi}m_0$ and the battery mass is $\frac{\phi}{1-\phi}m_0$.

We assume that the powertrain efficiency is constant and substitute (1), to obtain the following relation between the flight time, vehicle mass (m_0), and battery mass fraction:

$$T_{\text{flight}} \propto \frac{\frac{\phi}{1-\phi}m_0}{f_i^{\frac{3}{2}}} \propto \frac{\phi\sqrt{1-\phi}}{\sqrt{m_0}} \quad (3)$$

This relationship is plotted in Fig. 2, showing that vehicles with relatively small batteries expect to see a strong improvement in total flight time with increasing battery mass, until a peak where the battery takes up two thirds of the vehicle's mass. This large fraction makes structural design difficult and may lead to potential safety concerns. This analysis motivates our proposed system – by creating a system that enables the

multirotor to “shed” a discharged battery, and replace it with a fully charged battery, the vehicle is able to exceed the flight-time limitation imposed by (3).

III. DESIGN

In this section, we explain the design of the mid-air docking mechanism, the battery switching circuit, and the quadcopters used in our experiments.

A. Docking mechanism

Mid-air docking of multirotors has been performed using a variety of mechanisms in a variety of configurations. Robotic hands, a winch, and a rod were used by [13] to dock vehicles vertically aligned. Lateral docking using magnets has been demonstrated in [14]. Most of the existing designs either require additional actuators or rely on electromagnetic components, which adds to the complexity and vehicle weight. We required a fast docking procedure along with an easy undocking process. We decided to use a mechanical guide structure in the form of a landing platform on the main quadcopter and landing legs on the flying battery as shown in Fig. 3. This design achieves the following objectives:

- *No active components:* The mechanism does not consume power and uses the weight of the flying battery for docking. This makes it light-weight and leads to a simple undocking process – regular take-off.
- *Docks vertically aligned:* The flying battery does not produce any thrust when docked. Aligning the center of mass of the docked configuration along the thrust direction of the main quadcopter prevents unbalanced thrusts and additional power consumption.
- *Precision landing:* We require a secure electrical contact after docking to power the main quadcopter from the flying battery. This necessitates the electrical connectors to be well aligned.

The docking platform and the legs include electrical connectors which can allow the transfer of power from a flying battery to the main quadcopter. The docking mechanism allows some lateral play between the vehicles to facilitate smooth docking and undocking, but this play is limited sufficiently to ensure that the electrical connections are not broken due to vibrations and dynamic motions.

B. Battery switching circuit

One of the crucial features of our design is seamless switching from the primary battery to the secondary battery and back. Since our system is flying, we cannot afford to cut the power supply during this switch. The two batteries need to be connected in parallel for some time to achieve this. A direct parallel connection is only safe within a voltage difference of 0.2 V per cell for lithium polymer (LiPo) batteries. This would often not be the case in our application because we intend to utilize the secondary battery from a fully charged state (4.2 V per cell) to a completely discharged state (3.0 V per cell). We solve this by connecting diodes in series with each of the batteries to avoid reverse currents. We utilize smart bypass diodes because they have a much



Fig. 3: *Top*: Main quadcopter with the docking platform and spring loaded connectors. *Bottom*: Flying battery with the docking legs and copper plate connectors.

lower voltage drop than conventional P-N junction diodes or Schottky diodes. At our operating current of about 16 A, the voltage drop is less than 0.1 V.

A normally closed relay is connected in series with the primary battery. By opening the switch, we can draw power from the secondary battery even when it is at a lower voltage than the primary battery. The relay coil is connected to the secondary battery input leads in series with a MOSFET. This ensures that the switch does not turn off without a secondary battery, and allows us to use a GPIO pin on the flight controller to control the switch. Fig. 4 shows a schematic diagram of the battery switching circuit.

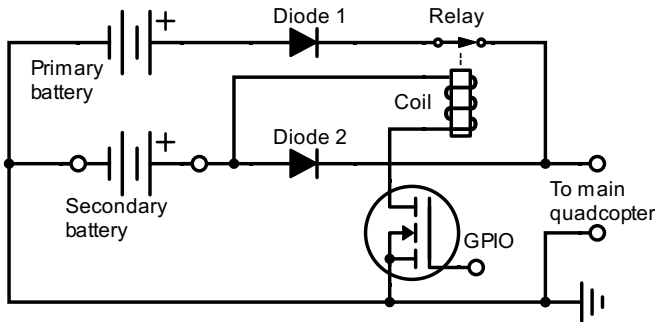


Fig. 4: Schematic of the battery switching circuit.

C. Vehicle design

1) *Main quadcopter*: The main quadcopter is designed to have enough payload capacity for carrying useful sensors such surveillance cameras, or environmental sensors.

TABLE I: Specifications of quadcopters used in experiments

Parameter	Main quadcopter	Flying battery
Propeller diameter	203 mm	76 mm
Arm length	165 mm	58 mm
Mass	820 g	320 g
Maximum thrust	27 N	8 N

TABLE II: Component masses

Component	Mass [g]
Primary battery	190.0
Secondary battery	135.0
Small quadcopter battery	45.0
Docking platform	45.0
Docking legs (each)	3.5
Battery switching circuit	60.0

The battery switching circuit and the docking platform are stacked on top of the main quadcopter. Spring-loaded connectors are mounted on the docking platform to serve as input leads to the quadcopter from the secondary battery. The primary battery is a 3S 2.2 Ah LiPo battery.

2) *Flying battery*: The small quadcopter was designed to have sufficient payload capacity to carry a secondary battery for the main quadcopter. The docking legs for the small quadcopter are designed to minimize blockage of the propeller airflow such that the payload capacity is minimally affected. Copper plates of dimensions similar to the spring-loaded connectors are installed on the legs to serve as the secondary battery output leads. The small quadcopter is powered using a 2S 0.8 Ah LiPo battery. The secondary battery is a 3S 1.5 Ah LiPo battery.

Table I summarizes the specifications of the vehicles used in our experiments. Masses of individual components are given in Table II.

IV. DOCKING MANEUVER

This section covers the considerations involved in docking and undocking the flying battery and the main quadcopter.

A. Aerodynamic disturbance rejection

A critical consideration for docking two quadcopters mid-air is the mutual aerodynamic interference caused by the airflow of the two vehicles. This consideration is especially important during vertical docking because one quadcopter is directly in the downwash of another. An analysis of rotorcraft downwash is presented in [15] and [16]. Detailed characterization and analysis of aerodynamic forces and torques between two quadcopters is shown in [17]. We will use the following key results from [17]:

- 1) The effect of mutual aerodynamic disturbances is primarily seen on the quadcopter that flies lower. The quadcopter that flies above is negligibly affected.
- 2) The predominant component of the aerodynamic forces is along the direction of the downwash. Forces perpendicular to the direction of the downwash can be ignored.

- 3) The aerodynamic torques disturb the bottom quadcopter in a way that tends to vertically align it with the top quadcopter. This is advantageous in our maneuver. Hence, we do not attempt to reject the torques.

We chose to fly the flying battery above the main quadcopter owing to result (1). The main quadcopter has sufficient thrust capacity to reject the disturbances caused by the flying battery's airflow. Based on results (2) and (3), the only disturbance that we correct for is the vertical force. This is done by applying a feedforward thrust based on the relative location of the two quadcopters.

The feedforward thrust map is created by flying the two quadcopters at various relative separations. A PID controller is used for position control which outputs a desired total thrust force. The feedforward thrust map is created from previous runs' controller integral actions, specifically creating a map of the required feedforward force for different positions.

B. Docking trajectory

The key requirement of this project is that the main quadcopter should not have to move substantially from its place during a long-term operation. Therefore, the docking trajectory involves minimal motion of the main quadcopter. Result (3) in Section IV-A mentions that aerodynamic torques tend to vertically align the two quadcopters. Based on this, we start by commanding the flying battery to go 30 cm vertically above the docking platform on the main quadcopter. It is then commanded to descend towards the docking platform. In this phase, any misalignments and tracking errors due to aerodynamic disturbances or other factors are corrected by the aerodynamic torque on the main quadcopter which restores the alignment.

Once the flying battery's center is within 2.0 cm radius of the docking platform's center in the horizontal plane and the bottom surface of its legs is within 3.0 cm of the platform's surface, it is commanded to free fall. The docking platform is designed to precisely align the flying battery's connectors with those on the main quadcopter once they are within a 2.0 cm radius in the horizontal plane. The drop height of 3.0 cm was chosen to have sufficient impact for the flying battery to slide in and align correctly, and also avoid rebounding which might cause misalignment. Fig. 1 shows a picture of the flying battery about to dock on the main quadcopter. Starting from takeoff, it takes about 20 s for the flying battery to dock on the main quadcopter. These distances and times were experimentally determined to give satisfactory results.

For the last phase, undocking, we command the flying battery to takeoff from the docking platform and go straight up to a position 30 cm above the platform. After this, the flying battery lands and another one is free to dock on the main quadcopter. The undocking maneuver takes approximately 8 s.

V. EXPERIMENTAL VALIDATION

We validate the use of our design by conducting an experiment involving repeated docking, battery switching,

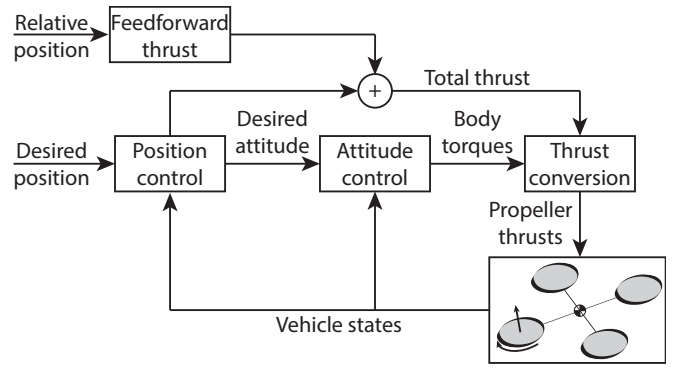


Fig. 5: Block diagram of the quadcopter controller. The flying battery does not have the feedforward thrust component.

and undocking so that the main quadcopter's use of the primary battery is only limited to the undocking and docking phases. Whenever the a flying battery is docked correctly, we use the secondary battery to power the main quadcopter.

A. Experimental setup

The quadcopters used in our experiments are localized via sensor fusion of a motion capture system and an onboard rate gyroscope. Experimental data from the motion capture system, voltage sensor, and current sensor are logged for post-processing via radio. We control the quadcopters using a cascaded PID position and attitude controller shown in Fig. 5. The integral action on the position and yaw helps prevent steady state errors and ensures that the vehicles are correctly vertically aligned. Additionally, feedforward thrust for the main quadcopter to reject aerodynamic disturbances is directly added to the total thrust based on the relative location of the flying battery with respect to the main quadcopter.

B. Demonstration

To demonstrate the ability and flight time benefit of our design, we conduct the following experiment:

- 1) The main quadcopter takes off with a fully charged primary battery hovers at a specific desired position.
- 2) A fully charged flying battery is commanded to dock on the main quadcopter.
- 3) Once docked, the main quadcopter switches its power source to the secondary battery and continues hovering.
- 4) Once the secondary battery is completely discharged, the main quadcopter switches back to the primary battery.
- 5) The flying battery is commanded to undock and land. Simultaneously, another fully charged flying battery takes off.
- 6) The second flying battery docks on the main quadcopter and we again switch the power source to the secondary battery.
- 7) During this period, we manually replace the discharged flying battery with a fully charged one.
- 8) This process is repeated until the primary battery of the main quadcopter, only consumed during the undocking and docking process, is completely discharged.



Fig. 6: Steps (4)-(6) of the demonstration. From left to right, (a) main quadcopter hovers with a flying battery docked on it, (b) the first flying battery is depleted, so it undocks and another fully charged flying battery takes off, (c) the second flying battery moves towards the main quadcopter to dock and first flying battery begins landing, (d) second flying battery descends to dock on the main quadcopter, (e) second flying battery is docked on the main quadcopter (which continues to hover) and first flying battery has landed - we now replace the discharged flying battery with a fully charged one.

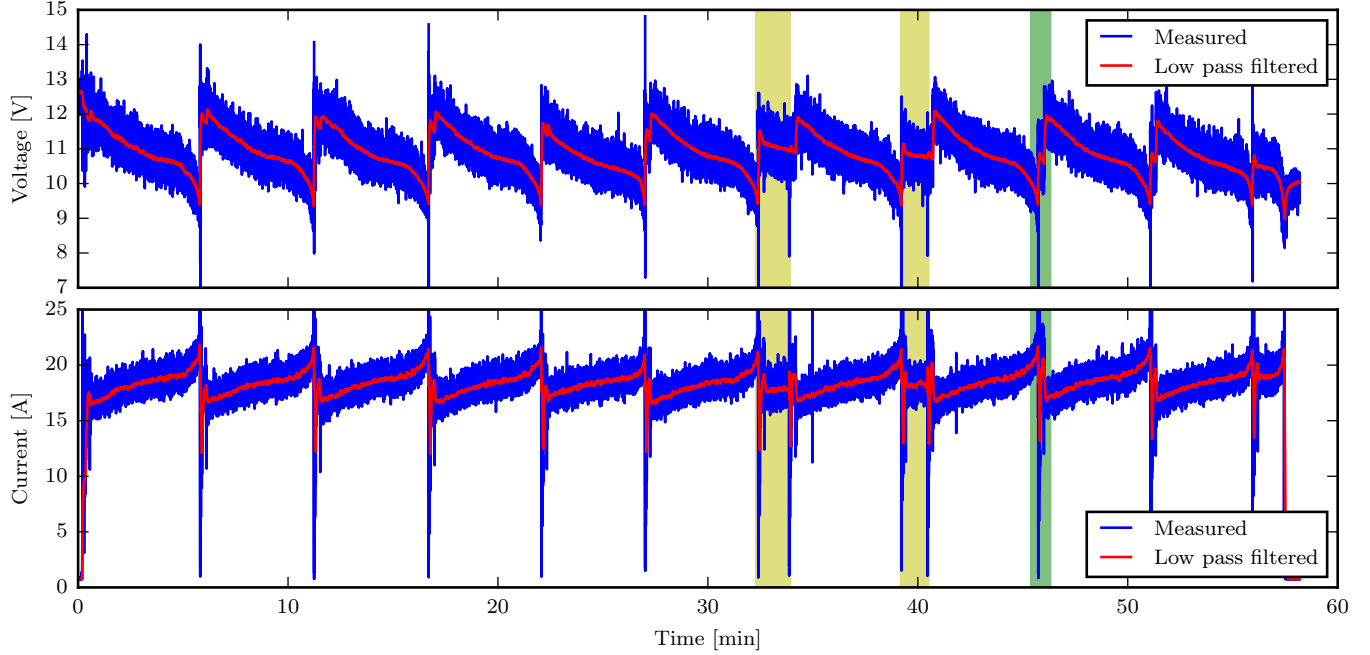


Fig. 7: Input voltage and current vs. time of the main quadcopter for the demonstration. Low pass filtered data has also been plotted for ease of visualization. The maximum current value of 55 A is cut off in the plot. Regions highlighted in yellow show parts of the experiment where the flying battery did not make electrical contact after docking. Fig. 8 shows a zoomed-in version of the green highlighted region

Fig. 6 shows steps (4)-(6) of the procedure. In this demonstration, the main quadcopter hovered for a total time of 57 min. The hovering time of the main quadcopter flying alone without the dock-switch-undock-repeat process was 12 min.

The plots of input voltage and current vs. time of the main quadcopter for the duration of the entire demonstration are shown in Fig. 7. We see the characteristic LiPo battery discharge curve [18] several times in the voltage vs. time plot. Each shows the complete energy consumption of one secondary battery. The current vs. time plot shows that current input to the quadcopter increases as the voltage decreases. This is expected because the power consumption of the quadcopter must remain approximately constant to hover continuously.

The regions in Fig. 7 highlighted in yellow show the parts of the experiment where the secondary battery did not connect to the circuit after docking. In those regions, the main quadcopter continues using the primary battery. We

command the incorrectly docked flying battery to undock and another fully charged flying battery to dock.

A typical undocking and docking maneuver part is highlighted in green on the plot and a zoomed-in version of that region is shown in Fig. 8. We see that when the main quadcopter switches back to the primary battery, the input voltage jumps to the primary battery voltage. When the relay is closed, the main quadcopter draws power from the battery which is at a higher voltage. After this the flying battery undocks. A temporary current and power surge is observed because the main quadcopter is now rejecting aerodynamic forces. This is followed the flying battery moving out and landing. In this part, the main quadcopter is flying without any additional mass or aerodynamic disturbance forces and hence we observe a dip in the power consumption. A few seconds later, another fully charged flying battery flies on top of the main quadcopter and begins descending to dock. We again observe an increase in power consumption because of aerodynamic disturbance rejection. Lastly, the flying battery

docks on the main quadcopter. Here we see another jump in voltage because the secondary battery is fully charged and at a higher voltage than the primary battery. Power consumption now settles around a value needed for hovering in the docked configuration.

From Table I the fraction of the main quadcopter's total mass from the battery is $\phi \approx 0.23$, with the vehicle's base mass $m_0 = 630\text{g}$. The vehicle's flight time is approximately 12 minutes. Referring to Fig. 2, this mass fraction corresponds to a total flight time of approx. 0.468 times the optimal flight time achievable for this vehicle. Thus, an "optimal" design would be capable of a maximum flight of 25.6 minutes; this design would however require a battery of 1.26kg for a total vehicle mass of 1.89kg, increasing the vehicle's overall weight by more than a factor 2. The flying battery concept is thus able to carry the vehicle payload for a flight more than twice as long as the theoretical limit for this base mass, while maintaining the vehicle total mass low, thus resulting in a safer, more useful vehicle. Finally, much more powerful drivetrain components (motors, ESCs) would be required to sustain flight at the increased mass, and clearly the vehicle would have much reduced maneuverability (due to dramatically reduced thrust-to-weight ratio).

VI. CONCLUSIONS

In this paper, we have introduced the concept and design of a flying battery - a small quadcopter that can carry a secondary battery for a main quadcopter, dock on it, and allow it to switch its power supply from the primary battery to the secondary battery.

We designed a passive docking mechanism in the form of a docking platform for the main quadcopter and docking legs on the small quadcopter to dock the two quadcopters mid-air. We also designed an onboard battery switching mechanism to seamlessly switch the power source of the main quadcopter from one battery to another and back mid-flight. This was achieved using various components including diodes to avoid backflow of current into batteries, a relay and MOSFET to turn the primary supply off and back on, and spring loaded connectors and copper plates to establish a secure electrical connection to draw power from the secondary battery.

We utilized an empirical model to provide a feedforward thrust from the main quadcopter to reject the aerodynamic disturbance forces on it due to the downwash of the flying battery above it.

Lastly, we demonstrated the ability of the system to dock, switch batteries, and undock multiple times in a single flight. This helped the main quadcopter achieve a flight time of 57 min as compared to its solo flight of 12 min. This is essentially a 4.7-fold increase in the flight time, and a $2.2\times$ increase over the theoretical flight time limit, all while keeping the vehicle in essentially the same safety class. This can be extremely useful in, for example, continuous monitoring activities.

A minor extension to this work would be redesigning the flying battery to only have a single battery, so that it flies using the secondary battery. This would reduce the vehicle

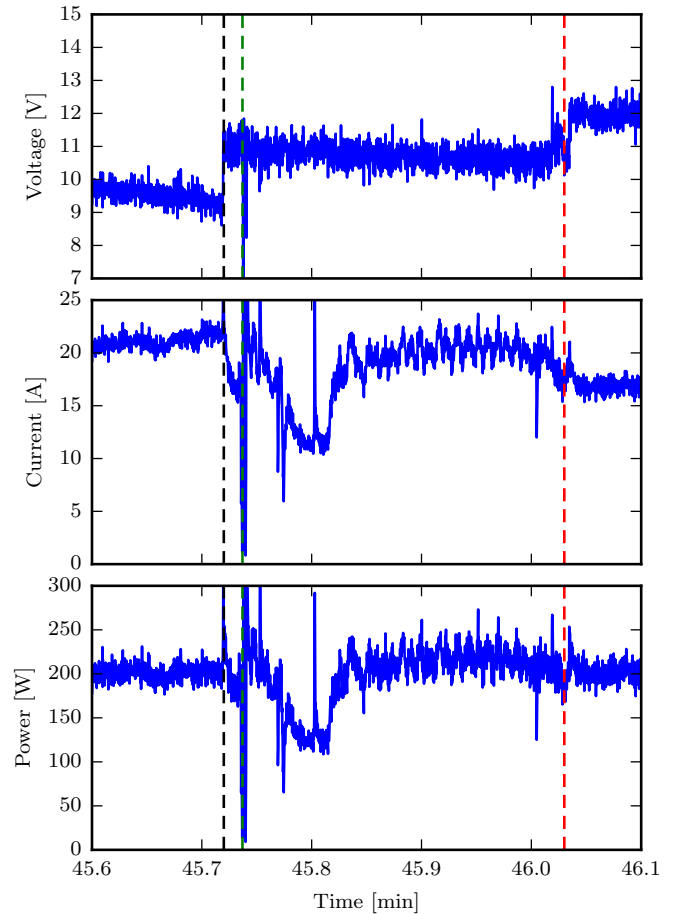


Fig. 8: Zoomed in version of the green highlighted region in Fig. 7 showing the input voltage, current, and power of the main quadcopter during undocking and docking. The dotted lines mark the following events: (i) black: main quadcopter switches to primary battery, (ii) green: the flying battery undocks, (iii) red: another flying battery docks.

mass, but would require some additional planning to ensure sufficient battery reserves for the flying battery to land.

Another extension is the exploration into the optimal use of the flying battery concept for range extension, including the more complex challenge of docking and undocking while the main quadcopter is moving.

A third extension is to use only on-board sensing for the docking, rather than relying on an external motion capture system as done in the demonstrations in this paper. This is obviously a crucial requirement for any practical deployment of the system, and would require careful design of the embedded sensing with the low-level planning during the sensitive docking and undocking maneuvers.

ACKNOWLEDGMENT

We gratefully acknowledge financial support from NAVER LABS. The experimental testbed at the HiPeRLab is the result of contributions of many people, a full list of which can be found at hiperlab.berkeley.edu/members/. The authors wish to acknowledge Minos Park for assisting with the experimental validation.

REFERENCES

- [1] S. Sharma, A. Muley, R. Singh, and A. Gehlot, "UAV for surveillance and environmental monitoring," *Indian Journal of Science and Technology*, vol. 9, no. 43, 2016.
- [2] S. Waharte and N. Trigoni, "Supporting search and rescue operations with UAVs," in *2010 International Conference on Emerging Security Technologies (EST)*. IEEE, 2010, pp. 142–147.
- [3] M. Erdelj, E. Natalizio, K. R. Chowdhury, and I. F. Akyildiz, "Help from the sky: Leveraging uavs for disaster management," *IEEE Pervasive Computing*, vol. 16, no. 1, pp. 24–32, 2017.
- [4] M. Boon, A. Drijfhout, and S. Tesfamichael, "Comparison of a fixed-wing and multi-rotor uav for environmental mapping applications: A case study," *The International Archives of Photogrammetry, Remote Sensing and Spatial Information Sciences*, vol. 42, p. 47, 2017.
- [5] H.-P. Thamm, N. Brieger, K. Neitzke, M. Meyer, R. Jansen, and M. Mönninghof, "Songbird—an innovative uas combining the advantages of fixed wing and multi rotor uas," *International Archives of the Photogrammetry, Remote Sensing & Spatial Information Sciences*, vol. 40, 2015.
- [6] A. Tagliabue, X. Wu, and M. W. Mueller, "Model-free online motion adaptation for optimal range and endurance of multicopters," in *2019 International Conference on Robotics and Automation (ICRA)*. IEEE, 2019, pp. 5650–5656.
- [7] A. Junaid, A. Konoiko, Y. Zweiri, M. Sahinkaya, and L. Seneviratne, "Autonomous wireless self-charging for multi-rotor unmanned aerial vehicles," *Energies*, vol. 10, no. 6, p. 803, 2017.
- [8] D. Lee, J. Zhou, and W. T. Lin, "Autonomous battery swapping system for quadcopter," in *2015 International Conference on Unmanned Aircraft Systems (ICUAS)*. IEEE, 2015, pp. 118–124.
- [9] T. Toksoz, J. Redding, M. Michini, B. Michini, J. P. How, M. Vavrina, and J. Vian, "Automated battery swap and recharge to enable persistent uav missions," in *AIAA Infotech@ Aerospace Conference*, vol. 21, 2011.
- [10] N. K. Ure, G. Chowdhary, T. Toksoz, J. P. How, M. A. Vavrina, and J. Vian, "An automated battery management system to enable persistent missions with multiple aerial vehicles," *IEEE/ASME transactions on mechatronics*, vol. 20, no. 1, pp. 275–286, 2014.
- [11] C. Holda, B. Ghalamchi, and M. W. Mueller, "Tilting multicopter rotors for increased power efficiency and yaw authority," in *2018 International Conference on Unmanned Aircraft Systems (ICUAS)*. IEEE, 2018, pp. 143–148.
- [12] B. W. McCormick, "Aerodynamics aeronautics and flight mechanics," 1995.
- [13] R. Miyazaki, R. Jiang, H. Paul, K. Ono, and K. Shimonomura, "Airborne docking for multi-rotor aerial manipulations," in *2018 IEEE/RSJ International Conference on Intelligent Robots and Systems (IROS)*. IEEE, 2018, pp. 4708–4714.
- [14] D. Saldana, B. Gabrich, G. Li, M. Yim, and V. Kumar, "Modquad: The flying modular structure that self-assembles in midair," in *2018 IEEE International Conference on Robotics and Automation (ICRA)*. IEEE, 2018, pp. 691–698.
- [15] D. Yeo, E. Shrestha, D. A. Paley, and E. M. Atkins, "An empirical model of rotorcraft uav downwash for disturbance localization and avoidance," in *AIAA Atmospheric Flight Mechanics Conference*, 2015, p. 1685.
- [16] S. Yoon, H. C. Lee, and T. H. Pulliam, "Computational analysis of multi-rotor flows," in *54th AIAA Aerospace Sciences Meeting*, 2016, p. 0812.
- [17] K. P. Jain, T. Fortmuller, J. Byun, S. A. Mäkiharju, and M. W. Mueller, "Modeling of aerodynamic disturbances for proximity flight of multirotors," in *2019 International Conference on Unmanned Aircraft Systems (ICUAS)*. IEEE, 2019, pp. 1261–1269.
- [18] N. Navarathinam, R. Lee, and H. Chesser, "Characterization of lithium-polymer batteries for cubesat applications," *Acta Astronautica*, vol. 68, no. 11-12, pp. 1752–1760, 2011.